

Supporting information

for New J. Chem.

Design of a high performance electrode composed of porous nickel-cobalt layered double hydroxide nanosheets supported on vertical graphene fibers for flexible supercapacitor

Yanping Song,^a Jixiang Zhang,^{*a} Nian Li,^{*b} Shuai Han,^{bc} Shihao Xu,^{bc} Fei jiang,^a Jun Yin,^a WanLi Qu^a, Cui Liu^b, Shudong Zhang^b and Zhenyang Wang^{*b}

- a. School of Mechanotronics & Vehicle Engineering, Chongqing Jiaotong University, Chongqing, China. Email: jxzhang@163.com
- b. Institute of Intelligent Machines, Chinese Academy of Sciences, Hefei, Anhui, China. Email: linain@issp.ac.cn; zywang@iim.ac.cn
- c. Department of Chemistry, University of Science & Technology of China, Hefei, Anhui, China.

1. Supporting Notes

Calculation of electrochemical performance:

The areal specific capacitance (C_A) of hybrid film electrodes, LIC-MSC and ACS device were calculated from galvanostatic charge/discharge curves as follows:

$$C_A = \frac{I \times \Delta t}{A \times \Delta V} \quad (1)$$

where C_A (mF/cm^2) is the areal specific capacitance, I (mA) is the discharge current, Δt (s) is the discharge time, ΔV (V) is the applied potential window, A (cm^2) is the area of electrodes. The charge balance of the ASC device is based on this formula:

$$\frac{A_+ \times H_+}{A_- \times H_-} = \frac{C_- \times V_-}{C_+ \times V_+} \quad (2)$$

where C (mF/cm^2) is the areal specific capacitance, V is the potential (V), A is the active area of electrode and H is the thickness of the electrode (Fig. S18†). Areal energy density E_A ($\mu\text{Wh/cm}^2$) and power density P_A ($\mu\text{W/cm}^2$) were calculated based on the equations:

$$E_A = \frac{C_A \times (\Delta V)}{2 \times 3600} \quad (3)$$

$$P_A = \frac{E_A \times 3600}{\Delta t} \quad (4)$$

where Δt is the discharge time, ΔV is the applied voltage.

The preparation of poly(vinyl alcohol) (PVA)/KOH gel electrolyte:

The mixture of 4g PVA ($M_w = 47\,000$, aladdin®) and 25 mL deionized water were stirred at 85 °C overnight, and 15 mL KOH solution (dissolved 4g KOH) was added into the mixture and stirred until the solution became homogeneous and transparent.

Flexible solid-state LIG-MSC fabrication:

The interdigitated electrodes of in-plane LIG-MSCs fabrication relied on laser irradiation patterning effect. And, conductive silver paste (MCN-DJ002, Mechanic) was applied on two joint parts of microelectrodes for better electrical contact. Copper tape was used to connect electrodes and an electrochemical workstation for testing. And, a kind of silicone (Wuqing® silicone, RTV704, Dongguan) was used to protect two joint parts of microelectrodes from electrolyte. The area of LIG-MSCs ($A_{\text{LIG-MSCs}}$) is the total area of the device including active interdigitated electrodes and the gaps between the electrodes. A LIG-MSCs is calculated as 2.73 cm^2 , considering 10 interdigitated electrodes with a width of 3.0 mm a length of 7.0 mm, and a spacing of 1.0 mm between two neighboring electrodes.

Preparation of AC/LIG electrode:

The activated carbon (80 wt%), acetylene black (10 wt%) and polyvinylidene fluoride (10 wt%) were fully mixed in NMP(N-Methyl pyrrolidone) to form a uniform slurry. Then, the slurry was coated on PPS-supported LIG sheet and dried at 80 °C for 12 h.

2. Supporting Figures

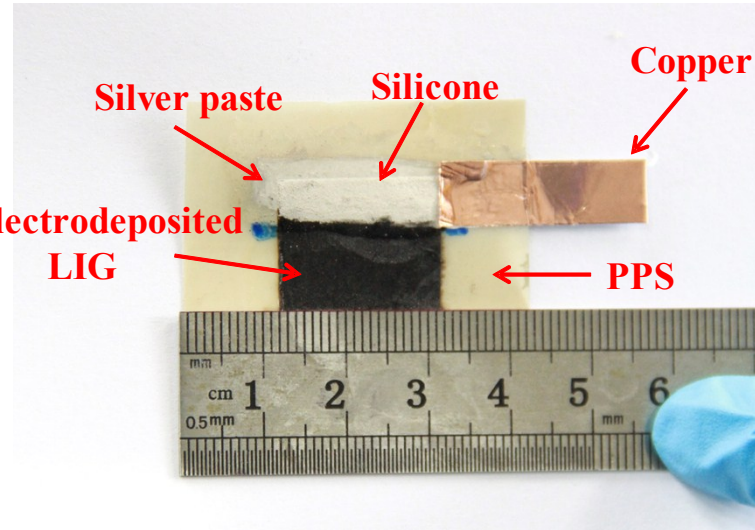


Fig S1 Photograph of a half-side electrode for ASC device.

Table S1. Comparisons of the I_D/I_G ratios of O-LIG and D-LIG at different laser powers in Fig.1a.

Laser power (W)	I_D/I_G ratio (O-LIG)	I_D/I_G ratio (D-LIG)
4.8	0.89	0.86
6.0	0.82	0.77
7.2	0.56	0.42

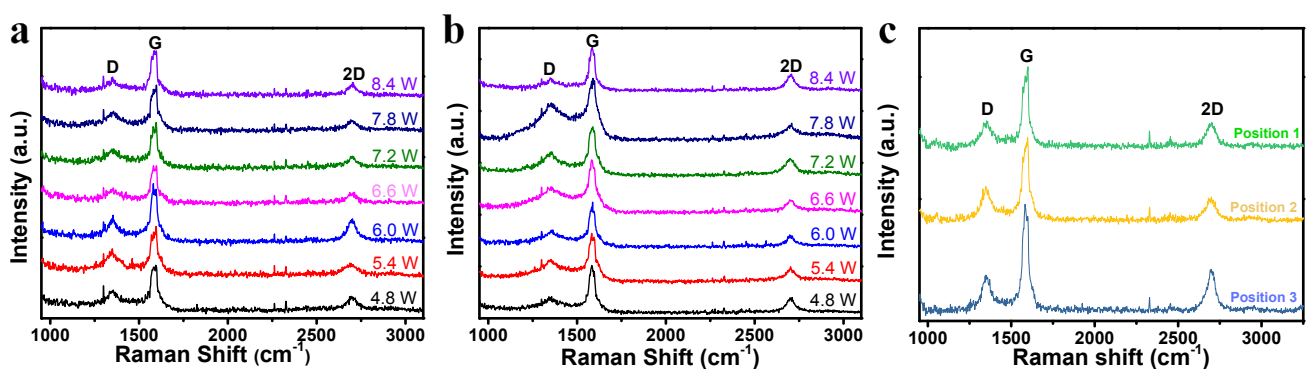


Fig. S2 Raman spectra of (a) O-LIG, (b) D-LIG and (c) different three positions in the same D-LIG sample.

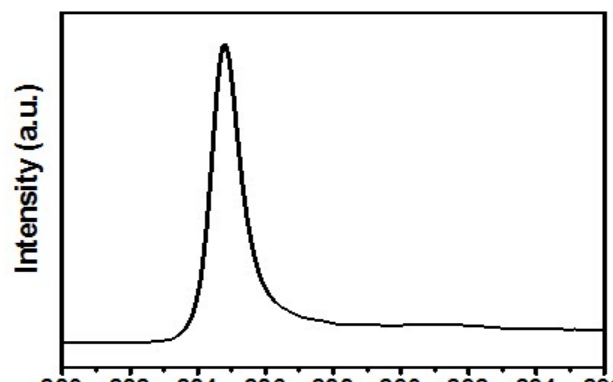


Fig. S3 High-resolution C 1s XPS spectrum of LIG.

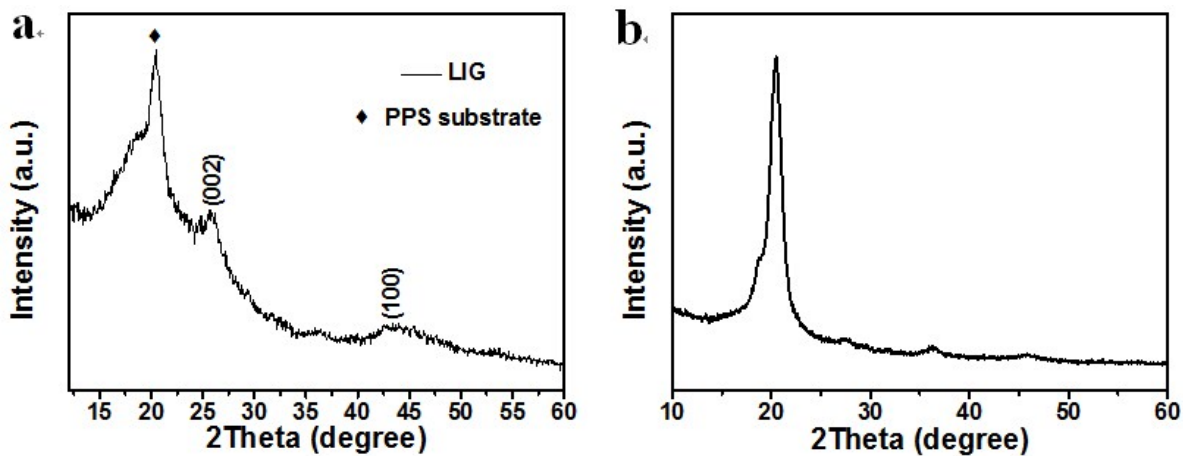


Fig. S4 The XRD patterns of (a) LIG and (b) PPS.

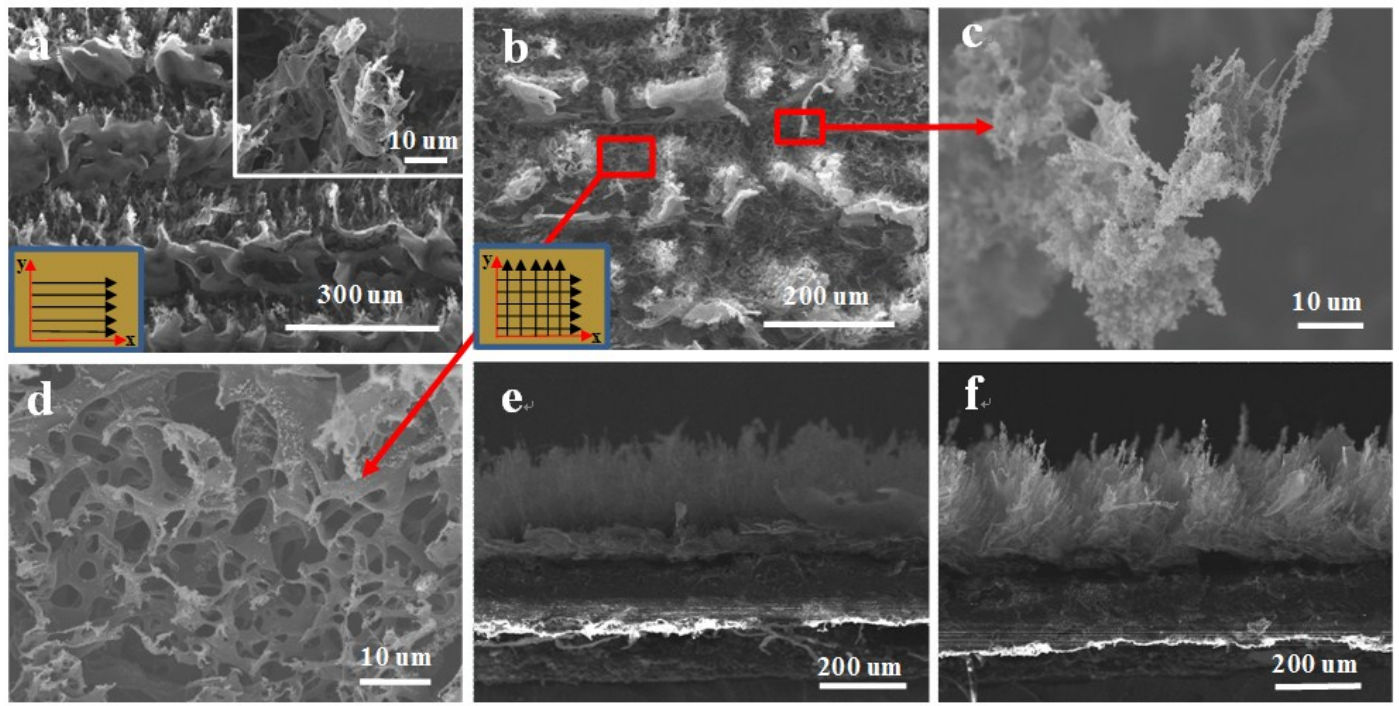


Fig. S5 The SEM images of O-LIG and D-LIG (a-d are different samples from Fig. 2): (a) SEM image of top view of O-LIG. The inset in (a) is the high-magnification SEM image of LIG. (b) SEM image of top view of D-LIG. (c) The high-magnification SEM image of the top of D-LIG fibers. (d) The high-magnification SEM image of the bottom of D-LIG fibers. (e-f) The local zoom images of in Fig. 1e and 1f (cross-sectional SEM images of O-LIG and D-LIG).

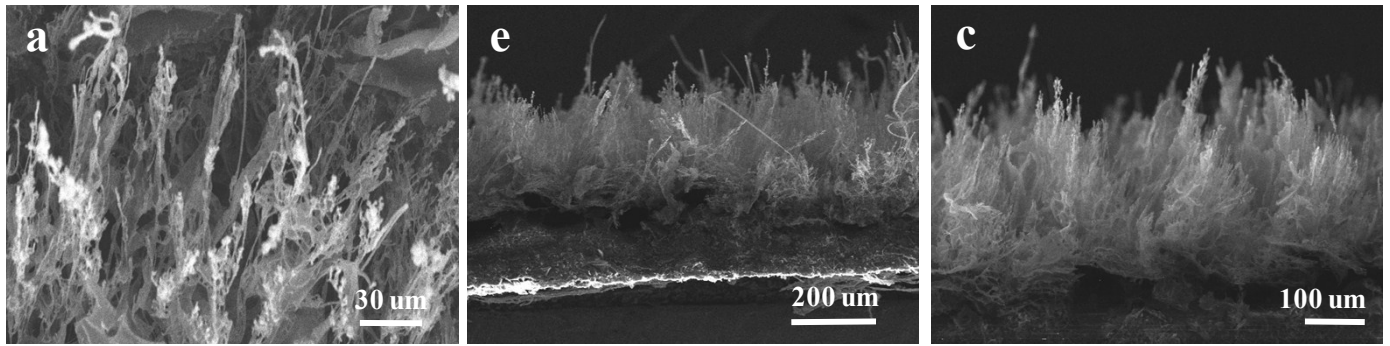


Fig. S6 (a) The SEM images of fibers structures of D-LIG. (e) and (c) The cross-sectional SEM images of fibers structures of D-LIG.

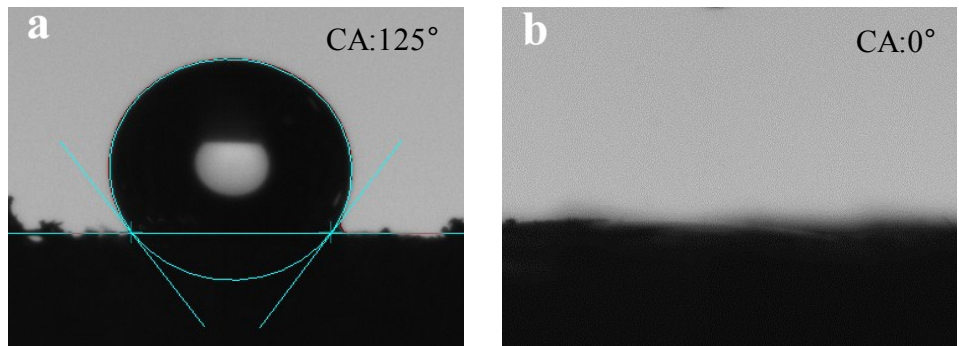


Fig. S7 (a) The contact angle of the pure LIG. (b) The contact angle of the as-made NC-LDH/LIG

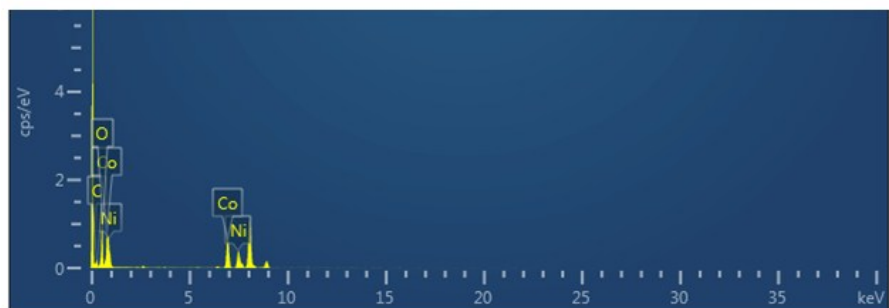


Fig. S8 The EDX spectrum of NC-LDHs/LIG.

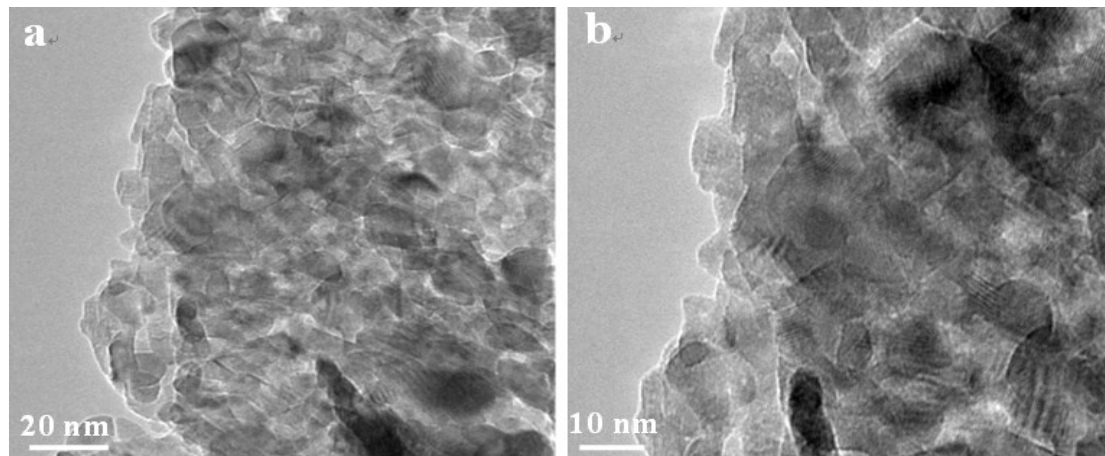


Fig. S9 The TEM images of NC-LDHs (a) at low magnification and (b) at high magnification. (The preparation of this sample without of HMT.)

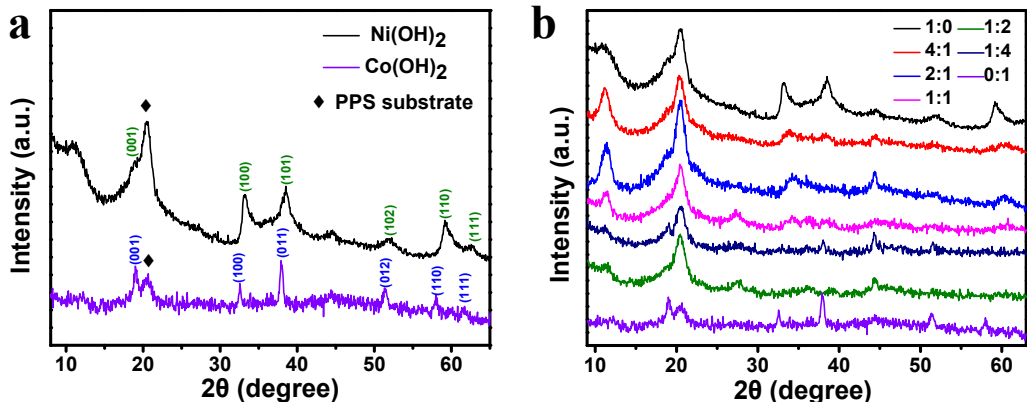


Fig. S10 (a) The XRD patterns of pure Ni and Co hydroxides (b) The comparison of XRD patterns of hybrid electrode with various Ni:Co feeding mole ratio.

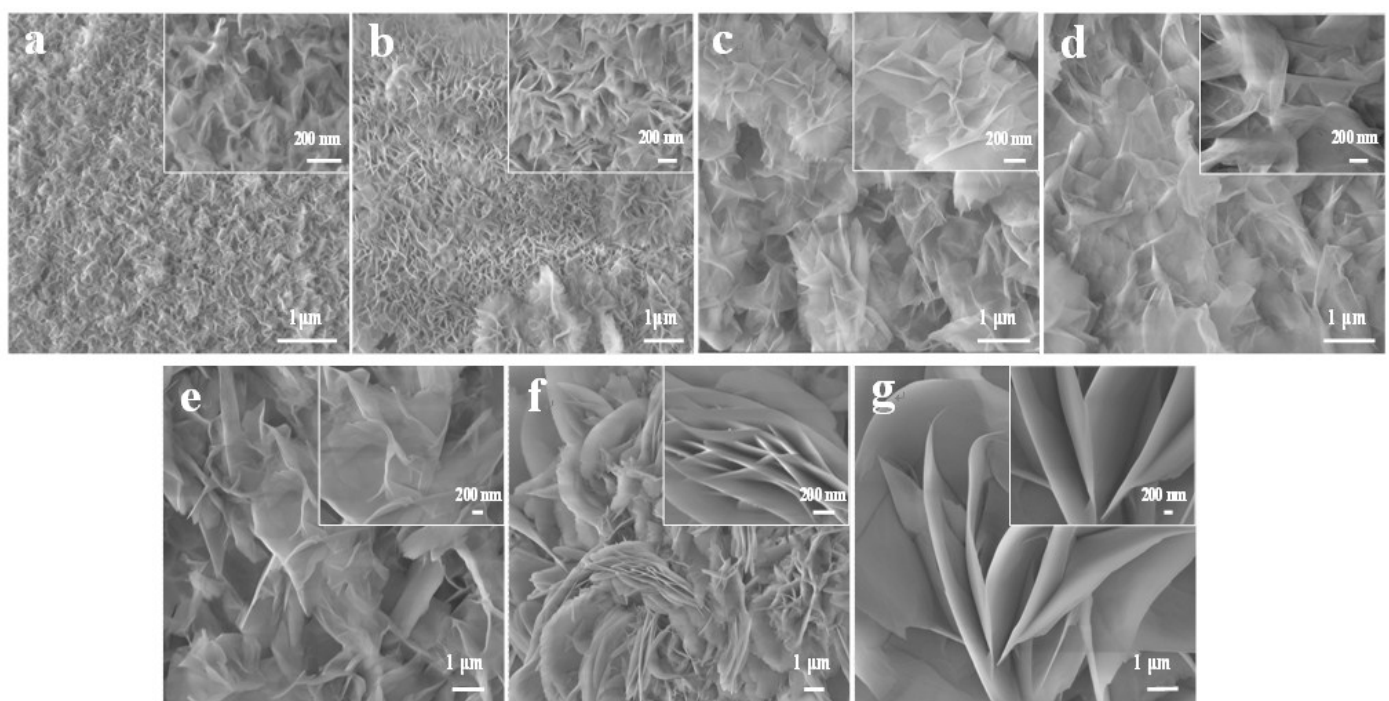


Fig. S11 SEM images of hydroxide nanosheets feeding with different mole ratios of Ni:Co: (a) 1:0. (b) 4:1. (c) 2:1. (d) 1:1. (e) 1:2. (f) 1:4. (g) 0:1.

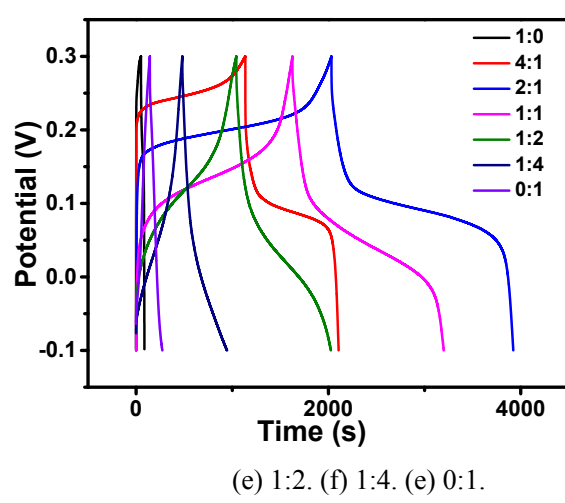


Fig. S12 GCD curves of the various Hydroxides/LIG hybrid electrodes at a current density of 1.0 mA/cm^2 .

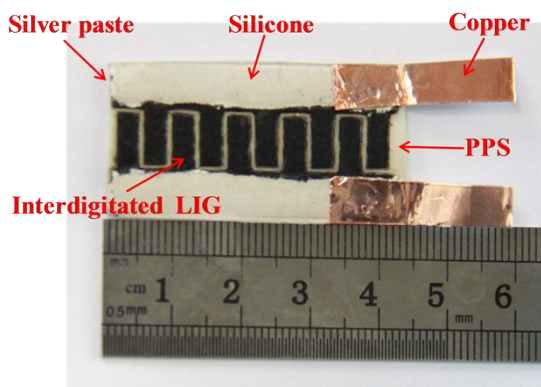


Fig. S13 Photograph of the interdigitated LIC-MSC.

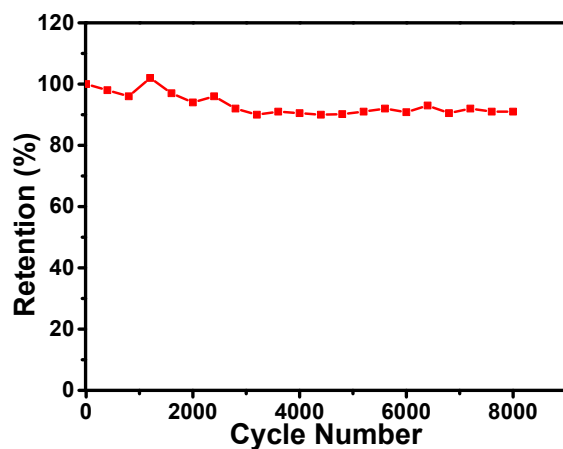


Fig. S14 The cycling performance at a current density of 0.1 mA/cm^2 of the LIG-MSC device.

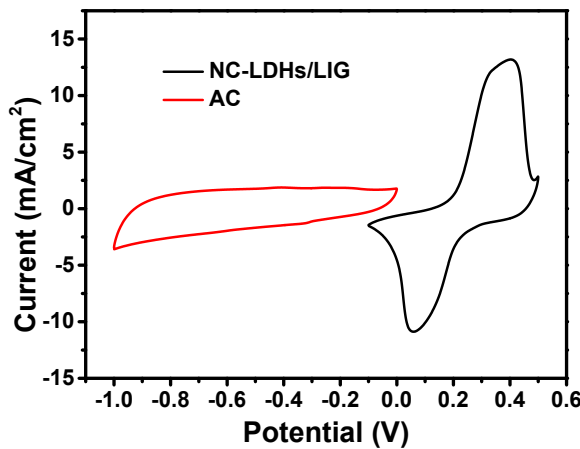


Fig. S15 The CV curves of NC-LDHs/LIG and AC/LIG electrode at scan rate of 2 mV/s.

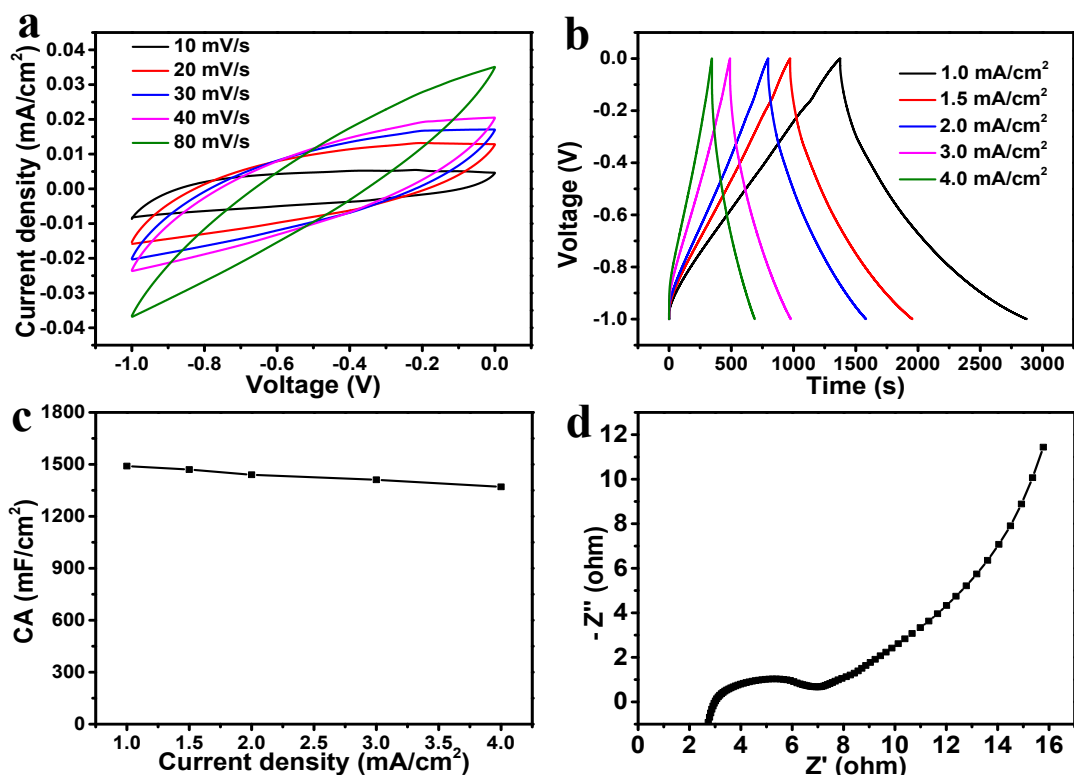


Fig. S16 The electrochemical properties of the AC/LIG electrode: (a) CV curves. (b) GCD curves. (c) The areal capacitance at various current densities and (d) Nyquist plot.

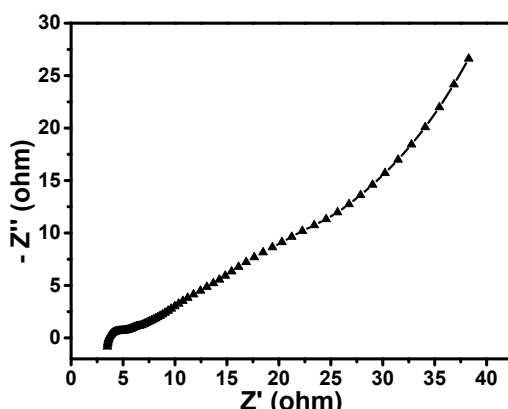


Fig. S17 Nyquist plot of NC-LDHs/LIG//AC device.

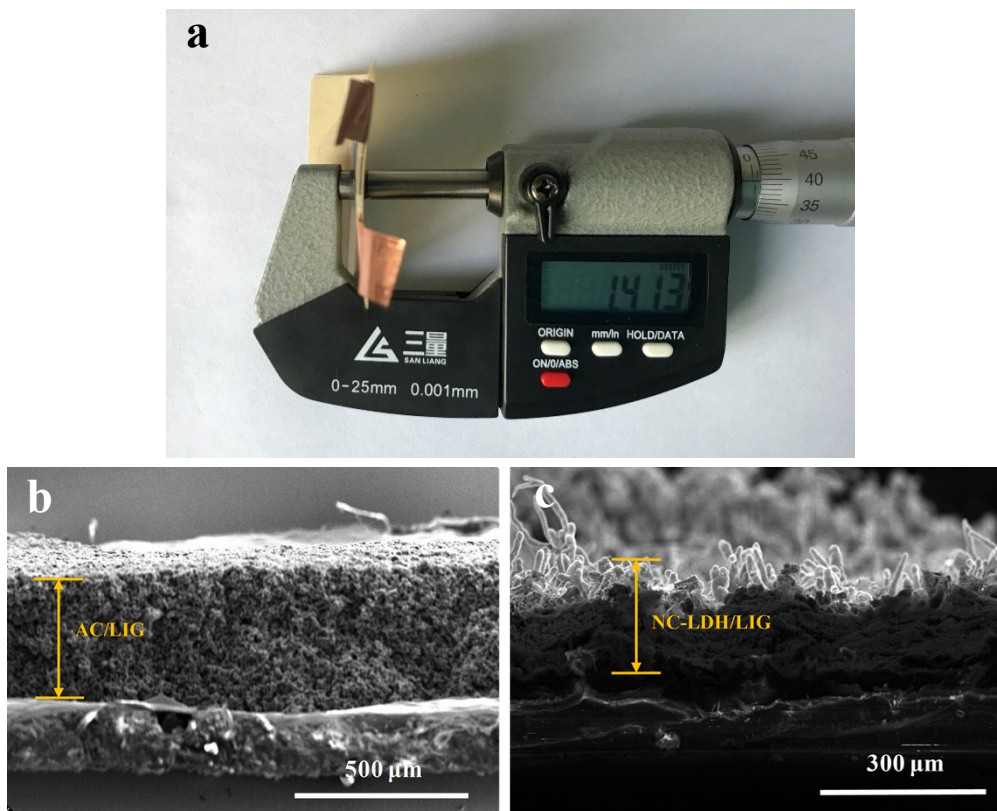


Fig. S18 (a) Photograph of the thickness of NC-LDHs/LIG//AC/LIG device. (b) The thickness of negative electrode (about 367 μm). (c) The thickness of positive electrode (about 204 μm).

Table S2. Comparisons of the specific capacitances for nickel-cobalt oxide/hydroxide electrode materials in a three-electrode system.

Active electrode materials	Electrolyte	Areal specific capacitance (mF/cm^2)	Ref.
NC-LDH NSs@Ag@CC	1 M KOH	1133 (1 mA/cm^2)	1
NC-LDH/NiCo ₂ O ₄	1 M KOH	1640 (2 mA/cm^2)	2
Ni _x Co _(1-x) (OH) ₂ /CNFP	1 M KOH	2030 (2.1 mA/cm^2)	3
NiCo ₂ O ₄	2 M KOH	3120 (1.11 mA/cm^2)	4

$\text{Co}_x\text{Ni}_{1-x}(\text{OH})_2/\text{NiCo}_2\text{S}_2$	1 M KOH	2860 (4 mA/cm ²)	5
$\text{ZnO}@\text{NiCo}_2\text{O}_4$	2 M KOH	3180 (6 mA/cm ²)	6
$\text{NiCo}_2\text{O}_4@\text{NiMoO}_4$	2 M KOH	2917 (2 mA/cm ²)	7
Ni-Co@Ni-Co LDH NTAs/CFC	1 M NaOH	2000 (4.6 mA/cm ²)	8

Table S3. Performance comparison of our ASC with some other sandwich-type supercapacitors.

Supercapacitor devices	Electrolyte	Areal specific capacitance (mF/cm ²)	Energy density (μWh/cm ²)	Power density (μW/cm ²)	Ref.
NC-LDH@Ag@CC//AC	1 M KOH	230.2(1 mA/cm ²)	78.8	785	¹
Symmetric NC-LDH@3D Ni/CC	PVA-KOH	439(1 mA/cm ²)	87.8	600	⁹
RGO/MnO ₂ //RGO	1 M Na ₂ SO ₄	113(10 mA/g)	35.1	37.5	¹⁰
Symmetric GO/PPy	1 M KCl	377.6(0.2 mA/cm ²)	16.8	80	¹¹
Symmetric CNT/PANI	H ₂ SO ₄ /PVA	184.6(1 mA/cm ²)	—	—	¹²
Symmetric β-Ni(OH) ₂ /graphene	PVA-KOH	61.7(5 mA/cm ²)	17	1200	¹³
Symmetric NiCo ₂ O ₄ nanowire	PVA-KOH	161(1 mA/cm ²)	—	—	¹⁴
Symmetric tea leaves	3 M KOH	640(1 mA/cm ²)	89	6100	¹⁵
NiCo ₂ O ₄ //AC	2 M KOH	380(1 mA/cm ²)	—	—	¹⁶
Co ₃ S ₄ @Ni ₃ S ₄ //porous carbon	2 M KOH	513(2 mA/cm ²)	190	1720	¹⁷
Symmetric CoNi ₂ S ₄ @NiSe@NF	6 M KOH	313(5mV/s)	31	—	¹⁸
NC-LDHs/LIG//AC/LIG	PVA-KOH	699.4(0.5 mA/cm ²)	219	2640	Our work

Notes: The highest energy density for NC-LDHs/LIG//AC/LIG device was obtained at 0.5 mA/cm² and the highest power density was calculated at 3.5mA/cm².

1. Sekhar, S. C.; Nagaraju, G.; Yu, J. S., Conductive silver nanowires-fenced carbon cloth fibers-supported layered double hydroxide nanosheets as a flexible and binder-free electrode for high-performance asymmetric supercapacitors. *Nano Energy* **2017**, *36*, 58-67.
2. Huang, L.; Chen, D. C.; Ding, Y.; Feng, S.; Wang, Z. L.; Liu, M. L., Nickel-Cobalt Hydroxide Nanosheets Coated on NiCo₂O₄ Nanowires Grown on Carbon Fiber Paper for High-Performance Pseudocapacitors. *Nano Letters* **2013**, *13* (7), 3135-3139.
3. Tuyen, N.; Boudard, M.; Joao Carmezim, M.; Fatima Montemor, M., NixCo_{1-x}(OH)(2) nanosheets on carbon nanofoam paper as high areal capacity electrodes for hybrid supercapacitors. *Energy* **2017**, *126*, 208-216.
4. Zhang, G. Q.; Wu, H. B.; Hoster, H. E.; Chan-Park, M. B.; Lou, X. W., Single-crystalline NiCo₂O₄ nanoneedle arrays grown on conductive substrates as binder-free electrodes for high-performance supercapacitors. *Energy & Environmental Science* **2012**, *5* (11), 9453-9456.
5. Xiao, J.; Wan, L.; Yang, S.; Xiao, F.; Wang, S., Design Hierarchical Electrodes with Highly Conductive NiCo₂S₄ Nanotube Arrays Grown on Carbon Fiber Paper for High-Performance Pseudocapacitors. *Nano Letters* **2014**, *14* (2), 831-838.

6. Zeng, W.; Wang, L.; Shi, H.; Zhang, G.; Zhang, K.; Zhang, H.; Gong, F.; Wang, T.; Duan, H., Metal-organic-framework-derived ZnO@C@NiCo₂O₄ core-shell structures as an advanced electrode for high-performance supercapacitors. *Journal of Materials Chemistry A* **2016**, *4* (21), 8233-8241.
7. Huang, L.; Zhang, W.; Xiang, J.; Xu, H.; Li, G.; Huang, Y., Hierarchical core-shell NiCo₂O₄@NiMoO₄ nanowires grown on carbon cloth as integrated electrode for high-performance supercapacitors. *Scientific Reports* **2016**, *6*.
8. Liu, Y.; Fu, N.; Zhang, G.; Xu, M.; Lu, W.; Zhou, L.; Huang, H., Design of Hierarchical Ni_xCo_{1-x} Layered Double Hydroxide Core-Shell Structured Nanotube Array for High-Performance Flexible All-Solid-State Battery-Type Supercapacitors. *Advanced Functional Materials* **2017**, *27* (8).
9. Li, Y.; Chen, J.; Ye, H.; Zhang, F.; Fu, X.-Z.; Sun, R.; Wong, C.-P., Hierarchical NiCo hydroxide nanosheets deposited on 3D porous Ni arrays for cost-effective high-performance supercapacitors. *Journal of Materials Science-Materials in Electronics* **2019**, *30* (3), 2552-2562.
10. Sumboja, A.; Foo, C. Y.; Wang, X.; Lee, P. S., Large Areal Mass, Flexible and Free-Standing Reduced Graphene Oxide/Manganese Dioxide Paper for Asymmetric Supercapacitor Device. *Advanced Materials* **2013**, *25* (20), 2809-2815.
11. Cao, J.; Wang, Y.; Chen, J.; Li, X.; Walsh, F. C.; Ouyang, J.-H.; Jia, D.; Zhou, Y., Three-dimensional graphene oxide/polypyrrole composite electrodes fabricated by one-step electrodeposition for high performance supercapacitors. *Journal of Materials Chemistry A* **2015**, *3* (27), 14445-14457.
12. Zeng, S.; Chen, H.; Cai, F.; Kang, Y.; Chen, M.; Li, Q., Electrochemical fabrication of carbon nanotube/polyaniline hydrogel film for all-solid-state flexible supercapacitor with high areal capacitance. *Journal of Materials Chemistry A* **2015**, *3* (47), 23864-23870.
13. Li, Y.; Ye, H.; Chen, J.; Wang, N.; Sun, R.; Wong, C.-P., Flexible beta-Ni(OH)₂/graphene electrode with high areal capacitance enhanced by conductive interconnection. *Journal of Alloys and Compounds* **2018**, *737*, 731-739.
14. Wang, Q.; Wang, X.; Liu, B.; Yu, G.; Hou, X.; Chen, D.; Shen, G., NiCo₂O₄ nanowire arrays supported on Ni foam for high-performance flexible all-solid-state supercapacitors. *Journal of Materials Chemistry A* **2013**, *1* (7), 2468-2473.
15. Bhoyate, S.; Ranaweera, C. K.; Zhang, C.; Morey, T.; Hyatt, M.; Kahol, P. K.; Ghimire, M.; Mishra, S. R.; Gupta, R. K., Eco-Friendly and High Performance Supercapacitors for Elevated Temperature Applications Using Recycled Tea Leaves. *Global challenges (Hoboken, NJ)* **2017**, *1* (8), 1700063-1700063.
16. Khalid, S.; Cao, C.; Wang, L.; Zhu, Y., Microwave Assisted Synthesis of Porous NiCo₂O₄ Microspheres: Application as High Performance Asymmetric and Symmetric Supercapacitors with Large Areal Capacitance. *Scientific Reports* **2016**, *6*.
17. Gao, Z.; Chen, C.; Chang, J.; Chen, L.; Wang, P.; Wu, D.; Xu, F.; Jiang, K., Porous Co₃S₄@Ni₃S₄ heterostructure arrays electrode with vertical electrons and ions channels for efficient hybrid supercapacitor. *Chemical Engineering Journal* **2018**, *343*, 572-582.
18. Tang, Z.; Jia, C.; Wan, Z.; Zhou, Q.; Ye, X.; Zhu, Y., Facile preparation of CoNi₂S₄@NiSe nano arrays on compressed nickel foam for high performance flexible supercapacitors. *Rsc Advances* **2016**, *6* (113), 112307-112316.